NEW INSIGHT IN OPERATION PRINCIPLES AND ACCURATE DESIGN OF FUNDAMENTAL AND HARMONIC MILLIMETER–WAVE OSCILLATORS

Matthias Curow

Arbeitsbereich Hochfrequenztechnik, Technische Universität Hamburg–Harburg,
Wallgraben 55, D–21071 Hamburg, Germany

Abstract

A new time–domain simulation method for design and optimization of millimeter–wave oscillators with Gunn and IMPATT devices is presented. The method allows load impedance functions of any complexity as calculated by mode–matching or other techniques to be used as input and is combined with an efficient and accurate hydrodynamic model for the active device. The operation principles of practical oscillator circuits are clarified. Results of this approach are compared with calculations based on impressed voltages and currents in order to determine the real power limits of GaAs Gunn oscillators.

1 Introduction

Efficient simulation tools are needed for an optimum design of millimeter–wave oscillators. In the past, a variety of different approaches using time–domain or frequency–domain techniques and various kinds of models for the active semiconductor device have been used successfully. However, some aspects of oscillator operation and optimum design are still not well understood, e. g. the possibly beneficial influence of package parasitics like the series resistance or inductance. The study of such effects require the use of accurate models for both the active device and the passive load which should still be numerically efficient to allow systematic investigations.

In this contribution, a new simulator is introduced which has been developed with respect to these requirements. The models for the active device, passive load structure, and their numerical implementation are briefly described. Some examples of results demonstrate that simulated systems behave very close to practical ones. In light of these results, the usefulness of simulations using impressed voltages or currents is discussed. It is shown that the former approach may be erroneous in case of harmonic Gunn oscillators since typical mounting structures enforce a current–driven operation at the fundamental frequency.

2 Models for active device and load impedance

When characteristic dimensions of semiconductor structures shrink, nonstationary carrier transport effects play an increasing role. This work focuses on GaAs Gunn elements and IMPATT diodes. In the millimeter–wave region, the drift–diffusion equations are often inappropriate. Instead, hydrodynamic (HD) models or Monte Carlo (MC) methods should be used. The main drawback of the latter approach is the large computational effort even using modern computers. Thus, the hydrodynamic model is a good compromise between the contrary requirements of accuracy, universality and computational efficiency.

Based on an unipolar version of the full hydrodynamic transport model as described already [1], a bipolar version has been developed. Special attention has been paid to the inclusion of the thermal energy [2] and the diffusive heat flow. Additional transport processes such as thermal generation, tunneling, and impact ionization are included. Values for ionization rates and other steady–state transport coefficients have been calculated by a MC code [3]. Since the parameterization of ionization coefficients may lead to incorrect breakdown and operating voltages, two separate energy balance equations for electrons and holes have been added to the model to remove the inconsistency regarding the MC data (valid for bulk material only) and their application to inhomogeneously doped structures. Results of the revised hydrodynamic model closely agree with those of several MC simulators and with measured results of Gunn and IMPATT oscillators.

For each simulated device, the thermal behavior of the semiconductor layers mounted on the heat sink and the resulting device temperature is taken into account. Devices were designed such that a conservative estimation of the temperature raise of 100 K only applies.

The impedance calculation of waveguide mounting structures is a very complex task. The present analysis is restricted to a widely used circuit consisting of a radial line resonator in a rectangular waveguide [4]. The radial line is formed by a pin and a disc; for simplicity, it is assumed that the active device is located on the waveguide bottom. A movable short allows an optimization of the output power. The load characte-

CH3577-4/95/0000-0545$01.00 © 1995 IEEE

ristic as seen at the semiconductor device package plane is calculated by mode–matching techniques. Results of two programs [5,6] have been found to be in very close agreement. Hence, in the frame of the validity of the approach, it can be assumed that calculated impedance characteristics are realistic.

The impedance transformation caused by the device package is modeled by a series resistance representing losses of semiconductor bulk and contact layers, and of the skin effect. Also, a series inductance and a parallel capacitance are considered. Although this lumped circuit cannot represent the actual transformation characteristic over a broader band, it is assumed that suitable values for the parasitics will lead to a correct impedance level at least in the frequency range of interest, i e. around the operating frequency. Note that a more accurate approach is possible using results of field analysis tools such as HP's HFSS for a complete three dimensional system formed by the waveguide, the resonator and the package.

3 Numerical procedures

The mathematical model consists of a set of 9 partial differential equations which are solved by a full implicit, decoupled, yet unconditionally stable finite–difference scheme which has been optimized for efficiency. Computation times are generally less than twice as high as for drift–diffusion calculations.

The load impedance is given as a table of frequency–dependent values. Since the time domain simulation of the active device needs already up to approx. 20 periods to reach the steady–state response to an impressed voltage (IMPATT diodes), a purely time–domain scheme for the inclusion of the interaction of the active device and the load impedance has been developed. The impulse response of the load characteristic is obtained from an inverse FFT (with typically 2^{15} — 2^{18} values). The convolution of this function with the time–dependent input signal gives the output response of the passive network in each time step which is used in turn to update the driving force for the active device. After a steady state is reached, the result is examined by means of Fourier analysis. Due to generally low quality factors of the networks, stable operation points are reached fast in most cases if they exist at all. Thus, total computation times are of order of a few minutes on an HP 720 RISC workstation.

4 Results

Up to now, harmonic Gunn and fundamental IMPATT oscillators with GaAs devices operating between 94 and 140 GHz have been examined. In the following, some typical results for systems at 94 GHz are given as examples.

An harmonic Gunn oscillator circuit according to [7] is examined since results of detailed measurements are available. Pin and disc diameter amount to 0.5 and 2 mm, respectively; the disc thickness is 0.2 mm, and the diameter and height of the package are 0.89 and 0.5 mm, respectively, representing a commercially packaged device (THOMSON CSF). The Gunn device is modeled as a flat–doped structure with a length of 1.8μm and a doping concentration of 10^{16}cm^{-3}. A bias voltage of 4.5 V is applied. A diameter of 65 μm leads to dissipation powers in the range 3 — 4 W and an operating temperature of 400 K on a copper heatsink.

The load impedance characteristic including the package transformation for different short positions and a comparison with a proposed equivalent circuit are shown in Figs. 1 and 2. Clearly, below the waveguide cutoff frequency f_c, the circuit behaves as a series resonant circuit with a real part given by the series loss resistance only. Hence, at the fundamental frequency $f_1 < f_c$, the device operates in a current–driven mode with a large fundamental component (see below). The short position does not affect the fundamental impedance and f_1 significantly, but shifts the parallel resonances so that keeping f_1 and the harmonic frequency f_2 nearly constant, different impedances at f_2 are provided with appropriate output power changes. It is obvious that large short distances may result in multi–mode operations which are known from practical experience to be unstable or less efficient, what is confirmed by simulation results.

Fig. 3 shows results for varying disc radii R. The fundamental frequency strongly depends on this parameter with a sensitivity $\Delta f_1/\Delta R \simeq -4$ GHz / 0.1 mm. This result gives an idea about the mechanical precision that is necessary for a reproductable oscillator design, especially for a power combining structure.

Disc thickness and pin diameter play a less important role, but suitable values may improve the performance through an optimized matching point at the fundamental frequency. Fig. 4 depicts that in this case, a thicker disc leads to a remarkable increase of the output power but at reduced frequencies.

The highest harmonic output powers have been found to be 30 — 40 mW in agreement with the measurements in [7] (typical values are close to 20 mW). Although the three parameters of the radial line have been systematically varied over broader ranges, no higher output powers have been found. However, reducing the package diameter and height to 0.7 and 0.4 mm, respectively, much higher powers of 100 mW are obtained as depicted in Fig. 5. Note that these results are fully covered by the measurements in [4], where simple flat–doped devices have been used, too. The reason for this power increase is a deeper minimum of the parallel resonance at 94 GHz, i. e. a reduced harmonic impedance level. Obviously, there is still some potential for power increase of commercial devices.

In order to systematically determine the power capabilities of the Gunn device, calculations with impressed sinusoidal voltages and currents have been performed for the first time for arbitrary phase shifts between the first and second harmonic component. Figs. 6 and 7 show some main results with bias voltage and operating temperature as before. Voltage–driven modes are less efficient than current–driven modes and require a higher impedance level. Very low dynamic resistances at f_1 as enforced in practical systems exclusively correspond to the latter mode. These figures allow a number of interesting conclusions regarding parametric effects to be drawn. Note that all results of con-

sistent simulations are covered by these data, and that the usual approach of representing the oscillator circuit by a voltage–driven operation of the active device with appropriate components fails to explain the highly efficient modes and power conversion mechanisms. It is expected that results for current driven modes indicate the real power limits of the device.

Due to the high harmonic output powers as measured in [4] and confirmed here, it is expected that the range of second harmonic power generation of GaAs Gunn devices extend well beyond 100 GHz. Preliminary results indicate that using commercial D–band IMPATT device packages, harmonic powers of more than 25 mW at 140 GHz are obtainable with 1.2 μm flat–doped devices.

Furthermore, a number of results regarding GaAs IMPATT oscillators are available. For example, simulated and measured output powers of 0.3 μm single–drift diodes [8] mounted with quartz stand–offs amount to 300 mW at 94 GHz. These results are reported in detail at the MTT Symposium.

5 Conclusion

A new simulator for the design and optimization of millimeter wave oscillators is introduced. It consists of an hydrodynamic transport model to analyze the semiconductor device combined with a realistic description of the frequency–dependent resonator configuration. The link of both parts in the time domain is established via a convolution method. Due to its ability to include impedance functions of any complexity, the simulator allows the examination of design aspects which are not covered so far by other and less accurate methods, for example such based on equivalent circuits.

6 Acknowledgement

The author is indebted to the Deutsche Forschungsgemeinschaft for financial support and to the authors of Refs. [5] and [6] for supplying their programs.

References

[1] M. Curow, A. Hintz. IEEE Trans. Electron Dev. ED–34 (1987) 1983–1994.

[2] M. Curow. Appl. Phys. Lett. 61 (1992) 2063–2065.

[3] S. J. J. Teng, R. E. Goldwasser. IEEE Electron Dev. Lett. 10 (1989) 412–414.

[4] P. Lugli. Microelectronic Eng. 19 (1992) 275–282.

[5] M. E. Bialkowski. AEÜ 38 (1984) 306–310.

[6] B. D. Bates, A. Ko. IEEE Trans. Microwave Theory Tech. 38 (1990) 1037–1045.

[7] H. Barth. Fortschrittberichte VDI Reihe 10 No. 8. Düsseldorf: VDI 1988.

[8] H. Eisele. Ph. D. Thesis, Technical University of Munich 1989.

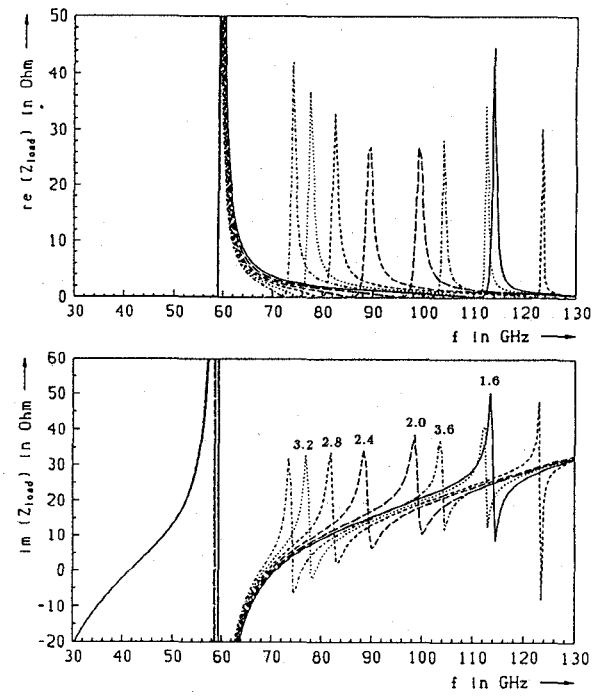

Fig. 1: Real and imaginary part of the impedance of the oscillator circuit according to [7] transformed by a series resistance and inductance of 0.2 Ω and 50 pH, respectively, and a parallel capacitance of 0.15 pH. The short positions are 1.6, 2.0, 2.4, 2.8, 3.2, and 3.6 mm.

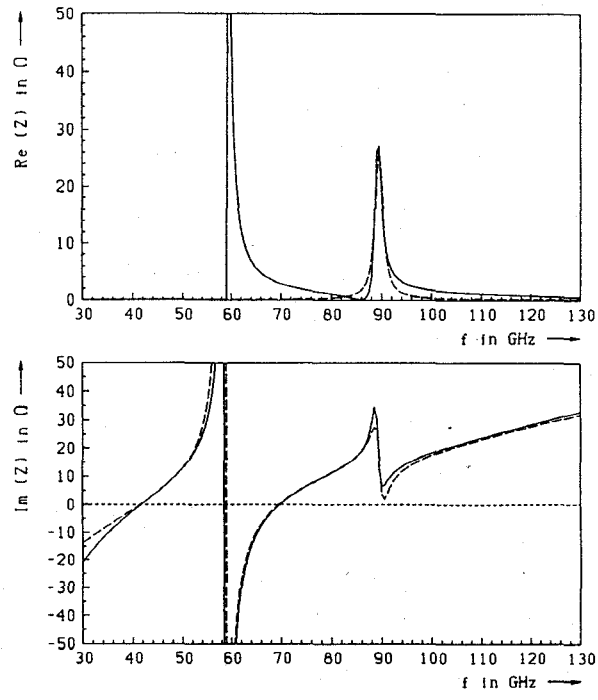

Fig. 2: Load impedance of the oscillator circuit as given by the mode–matching technique (——) and of an equivalent circuit (– – –) which consists of a series resonant circuit in series with a lossless and a lossy parallel resonant circuit; the Q–factor of the latter is 50.

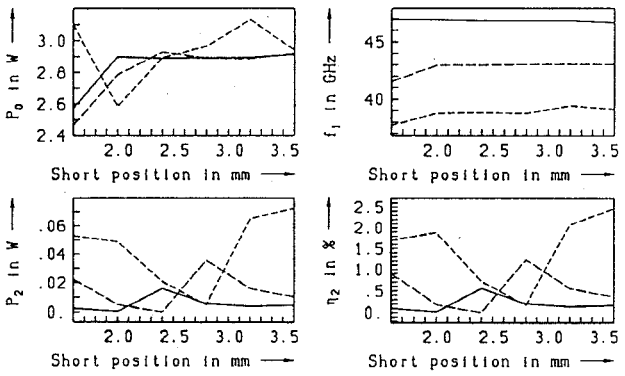

Fig. 3: DC power, fundamental frequency, and second harmonic power and efficiency for three different disc radii of 1.02 (——), 1.12 (– – –), and 1.22 mm (- - - -).

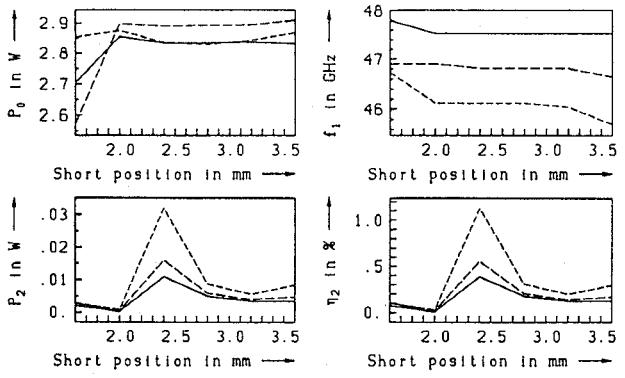

Fig. 4: Same parameters as in Fig. 3 for three different disc thicknesses of 0.1 (——), 0.2 (– – –), and 0.3 mm (- - - -).

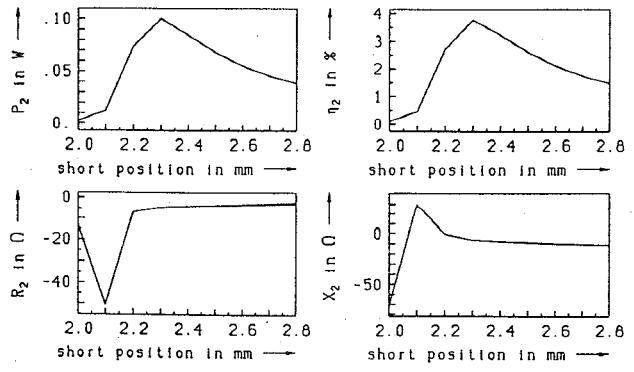

Fig. 5: Second harmonic power, efficiency, resistance, and reactance for an optimized package with a diameter of 0.7 mm and a height of 0.4 mm.

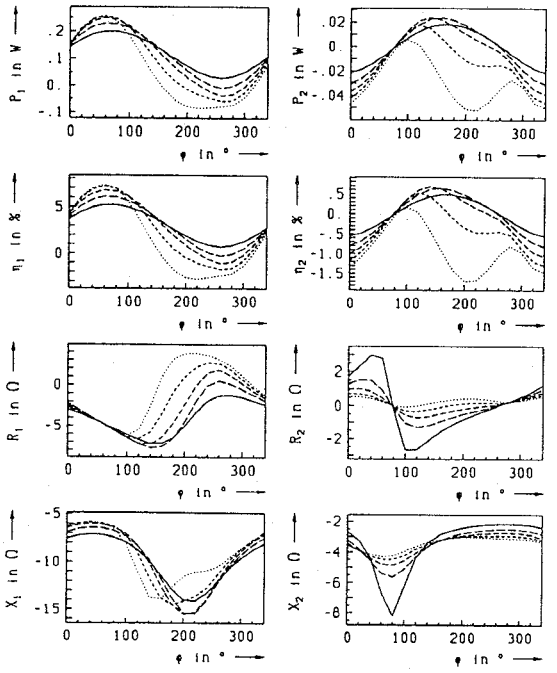

Fig. 6: Output power, efficiency, and dynamic resistance and reactance of the Gunn device at fundamental and harmonic frequencies 47/94 GHz for a varying phase shift φ of the second harmonic component against the fundamental one. Impressed voltages with a fundamental magnitude of 2.5 V and 5 different harmonic magnitudes in the range 0.5 — 1.5 V in steps of 0.25 V were used. The lowest magnitude corresponds to solid lines and the highest to dash–dotted lines.

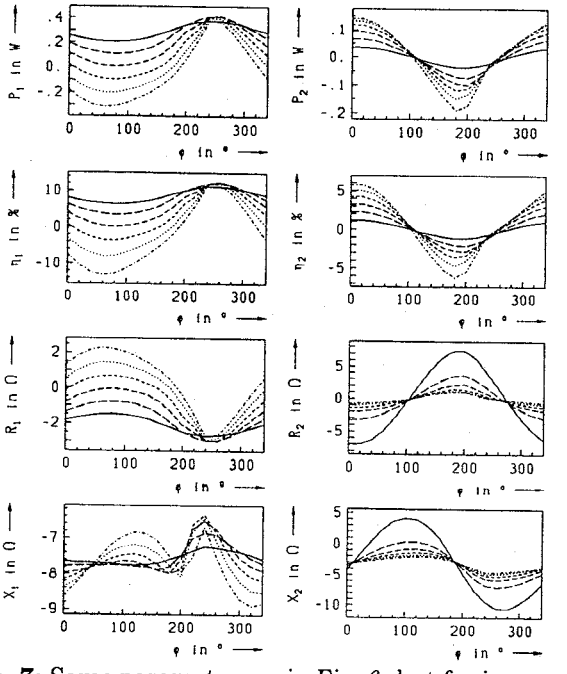

Fig. 7: Same parameters as in Fig. 6, but for impressed currents with a fundamental magnitude of 0.5 A and 6 different harmonic magnitudes in the range 0.1 — 0.6 A in steps of 0.1 A.